






# An interferon gamma response signature links myocardial aging and immunosenescence

DiyaaEIDin Ashour<sup>1,2</sup>, Sabine Rebs<sup>3</sup>, Panagiota Arampatzi <sup>4</sup>,  
Antoine-Emmanuel Saliba <sup>5,6</sup>, Jan Dudek<sup>2</sup>, Richard Schulz<sup>7</sup>, Ulrich Hofmann<sup>1,2</sup>,  
Stefan Frantz <sup>1,2</sup>, Clément Cochain <sup>2,8</sup>, Katrin Streckfuß-Bömeke<sup>3,9</sup>,  
and Gustavo Campos Ramos <sup>1,2\*</sup>

<sup>1</sup>Department of Internal Medicine I, University Hospital Würzburg, Oberdürrbacher Str. 6, 97080 Würzburg, Germany; <sup>2</sup>Comprehensive Heart Failure Centre, University Hospital Würzburg, Am Schwarzenberg 15, 97078 Würzburg, Germany; <sup>3</sup>Institute of Pharmacology and Toxicology, University of Würzburg, Versbacher Str. 9, 97078 Würzburg, Germany; <sup>4</sup>Core Unit Systems Medicine, University of Würzburg, Josef-Schneider-Str. 2, 97080 Würzburg, Germany; <sup>5</sup>University of Würzburg, Faculty of Medicine, Institute of Molecular Infection Biology (IMIB), Josef-Schneider-Str. 2, 97080 Würzburg, Germany; <sup>6</sup>Helmholtz Institute for RNA-based Infection Research (HIRI), Helmholtz-Centre for Infection Research (HZI), Josef-Schneider-Str. 2, 97080 Würzburg, Germany; <sup>7</sup>Departments of Pediatrics and Pharmacology, Mazankowski Alberta Heart Institute, University of Alberta, 4-62 HMRC, 11207 87 Ave NW, Edmonton, Alberta T6G, 2S2 Canada; <sup>8</sup>Institute of Experimental Biomedicine, University Hospital Würzburg, Josef-Schneider-Str. 2, 97080 Würzburg, Germany; and <sup>9</sup>Clinic for Cardiology and Pneumology, Georg-August University Göttingen, and DZHK (German Centre for Cardiovascular Research), Robert-Koch-Straße 40, 37075 Göttingen, Germany

Received 26 October 2022; revised 24 January 2023; accepted 21 February 2023; online publish-ahead-of-print 4 May 2023

**Time of primary review: 24 days**

## Aims

Aging entails profound immunological transformations that can impact myocardial homeostasis and predispose to heart failure. However, preclinical research in the immune-cardiology field is mostly conducted in young healthy animals, which potentially weakens its translational relevance. Herein, we sought to investigate how the aging T-cell compartment associates with changes in myocardial cell biology in aged mice.

## Methods and results

We phenotyped the antigen-experienced effector/memory T cells purified from heart-draining lymph nodes of 2-, 6-, 12-, and 18-month-old C57BL/6J mice using single-cell RNA/T cell receptor sequencing. Simultaneously, we profiled all non-cardiomyocyte cell subsets purified from 2- to 18-month-old hearts and integrated our data with publicly available cardiomyocyte single-cell sequencing datasets. Some of these findings were confirmed at the protein level by flow cytometry. With aging, the heart-draining lymph node and myocardial T cells underwent clonal expansion and exhibited an up-regulated pro-inflammatory transcription signature, marked by an increased interferon- $\gamma$  (IFN- $\gamma$ ) production. In parallel, all major myocardial cell populations showed increased IFN- $\gamma$  responsive signature with aging. In the aged cardiomyocytes, a stronger IFN- $\gamma$  response signature was paralleled by the dampening of expression levels of transcripts related to most metabolic pathways, especially oxidative phosphorylation. Likewise, induced pluripotent stem cells-derived cardiomyocytes exposed to chronic, low grade IFN- $\gamma$  treatment showed a similar inhibition of metabolic activity.

## Conclusions

By investigating the paired age-related alterations in the T cells found in the heart and its draining lymph nodes, we provide evidence for increased myocardial IFN- $\gamma$  signaling with age, which is associated with inflammatory and metabolic shifts typically seen in heart failure.

## Keywords

Cardiac aging • T cells • Interferon gamma • Heart failure and immune cells

\* Corresponding author. Immunocardiology Lab, Comprehensive Heart Failure Centre (CHFC), Am Schwarzenberg 15, 97078 Würzburg. Tel: +49 931 201 46477; fax: +49 931 201 46485, E-mail: Ramos\_G@ukw.de

© The Author(s) 2023. Published by Oxford University Press on behalf of the European Society of Cardiology.

This is an Open Access article distributed under the terms of the Creative Commons Attribution-NonCommercial License (<https://creativecommons.org/licenses/by-nc/4.0/>), which permits non-commercial re-use, distribution, and reproduction in any medium, provided the original work is properly cited. For commercial re-use, please contact [journals.permissions@oup.com](mailto:journals.permissions@oup.com)

# 1. Introduction

The prevalence of myocardial diseases increases sharply with age, but most preclinical research in cardiology is conducted in young healthy animals. In Germany, for example, the average age of first myocardial infarction onset is 66.6 and 75.3 in men and women, respectively.<sup>1</sup> Likewise, the prevalence of heart failure increases from less than 1% among patients ageing 45–55 years to over 10% among octogenarians. In elderly patients, myocardial diseases are often accompanied by diverse comorbidities and frailty, which overall can impact the prognosis and therapy success.

The crosstalk between the immune and cardiovascular systems has come more into focus over the past few decades,<sup>2</sup> and the immune system also undergoes profound changes during the aging process.<sup>3,4</sup> This is manifested by a reduction in the thymic output of naive T cells,<sup>5</sup> a skewing of the adaptive T cell receptor (TCR) repertoire diversity in response to life-long exposure to chronic infections.<sup>6</sup> Additionally, haematopoietic stem cells accumulate somatic mutations, giving rise to clones that have a higher pro-inflammatory signature.<sup>7</sup> These changes in the immune system, with increased baseline low-grade inflammation, have been termed ‘inflammaging’<sup>3</sup> and have been associated to worsened response to infection,<sup>8</sup> and reduced vaccine efficacy.<sup>9</sup> Simultaneously, aging is characterized by a worsened wound healing capacity,<sup>10</sup> and adverse remodelling after myocardial injury compared to young individuals.<sup>11</sup>

A potential link between aging of the immune system and cardiovascular health has been suggested.<sup>12</sup> Previously, we showed that physiological myocardial aging is accompanied by an increased inflammatory response in the heart. This is reflected by a shift in T cells in the heart draining mediastinal lymph nodes towards an effector, pro-inflammatory cytokine-releasing profile. Other studies have computed scoring metrics to assess the aging of the immune system and its correlation with increased cardiovascular disease risk.<sup>13,14</sup> A reduction in the naive T cell pool and an increase in CD57<sup>+</sup> highly differentiated T cells were among the strongest predictors of an increase in cardiovascular events.<sup>13</sup> Additionally, chronic viral infections such as the cytomegalovirus, which are associated to accelerated immunological senescence profile, have been linked to increased cardiovascular risk and mortality, and with more advanced heart failure.<sup>15</sup> Yet, a clear distinction of the roles played by the immune cell subsets in the aging heart is yet to be established.

In the present study, we used single-cell transcriptomics, single-cell T cell repertoire analyses, and multi-colour flow cytometry to characterize how the murine heart and its draining lymph nodes change side-by-side with aging. Simultaneously, we profiled the non-cardiomyocyte cell subsets from 2- to 18-month-old hearts. Our data revealed an age-dependent increase in T cell-derived IFN- $\gamma$  signalling in the heart and its draining lymph nodes, which promotes low-grade inflammation and metabolic rewiring in the aged heart.

# 2. Methods

## 2.1 Animals and study approval

Physiological aging was studied in naive male and female C57BL/6J mice aged 2, 6, 12, or 18 months acquired from the Jackson Laboratory and housed under specific pathogen-free conditions, with a controlled light–dark cycle and a standard diet. All animal procedures were approved by the local authorities (Regierung von Unterfranken) and conformed to the guidelines from Directive 2010/63/EU of the European Parliament on the protection of animals used for scientific purposes.

## 2.2 Ex vivo analyses

Animals were sacrificed by cervical dislocation and then perfused with phosphate buffered saline -heparin (50 IU/mL) to flush the coronary circulation and remove blood-borne leucocytes, according to a described protocol.<sup>16</sup> Depending on the experimental setup, mediastinal, popliteal, and mesenteric lymph nodes, spleen, heart, lung liver, and hind limb skeletal muscle were harvested, and blood was drawn from the cheek as previously

described.<sup>17</sup> Single-cell suspensions were prepared from the different organs to be used for flow cytometry or magnetic cell sorting for single-cell sequencing (sc-seq) purposes. A detailed description of all procedures is provided in [Supplemental Methods](#).

## 2.3 Single-cell RNA-sequencing

Single-cell RNA-sequencing was performed using a 10 $\times$  Genomics platform (Pleasanton, CA, USA). Libraries generated were sequenced using the NovaSeq 6000 platform (S2 Cartridge, Illumina, San Diego, CA, USA). Raw data were processed using the Cell Ranger Software Suite (10 $\times$  Genomics, Pleasanton, CA, USA), and downstream analyses were performed using different R packages. A more detailed explanation for the sc-seq experiment is found in the [Supplemental Methods](#).

## 2.4 Induced pluripotent stem cells-derived cardiomyocyte cultures

Induced pluripotent stem cell (iPSC) derived cardiomyocytes were generated as previously described,<sup>18</sup> followed by treatment with 10 IU/mL IFN- $\gamma$  for either 1 or 4 weeks. After treatment period, cells were assessed by immunofluorescence microscopy and by Seahorse Extracellular flux Analyzer (Seahorse Bioscience, Billerica, MA, USA) for measuring cellular metabolism. Detailed protocols can be found in the [Supplemental Methods](#).

## 2.5 Statistical analyses

Unless otherwise stated, the results are presented as the mean  $\pm$  standard error of the mean (SEM) along with the distribution of all individual values in each group. The sample size for each group is described in each graph legend. The statistical analyses were performed with GraphPad Prism (version 7.0 or 9.0.0, GraphPad Software, San Diego, CA, USA), as described in the figures' legends. Differences were considered significant when  $P < 0.05$ .

# 3. Results

## 3.1 Single-cell sequencing analysis of heart and T cells in heart draining mediastinal lymph node simultaneously

C57BL/6J male and female mice of ages 2, 6, 12, and 18 months were used to dissect the kinetics of T cell aging and their impact on cardiac tissue inflammation during the process of physiological aging ([Figure 1A](#)). There was a linear increase in heart and body weight of the animals both in males and females along the aging axis (see [Supplementary material online, Figure S1](#)). We sorted CD4<sup>+</sup> and CD8<sup>+</sup> T cells with an effector and/or memory phenotype, including both central memory (CD62L<sup>+</sup> CD44<sup>high</sup>) and effector cells (CD44<sup>high</sup> CD62L<sup>−</sup>) from the heart draining mediastinal lymph nodes (see [Supplementary material online, Figure S2A, Supplementary material online, Table S1](#)) and performed sc-seq using 5' technology from the 10 $\times$  Genomics platform. This enabled us to simultaneously characterize the gene expression profile of each T cell together with its antigen receptor variable regions (encompassing the V, D, and J gene segments).

To avoid batch effects, sorted mediastinal lymph node T cells of different age groups were labelled with Totalseq-C hashtag antibodies, sequenced together and, de-multiplexed *in silico* (see [Supplementary material online, Figure S3](#)). Additionally, from the same 2- and 18-month-old male and female C57BL/6J mice, we sorted the different non-cardiomyocyte subsets using an adjusted strategy from Skelly *et al.* (see [Supplementary material online, Figure S2B, Supplementary material online, Table S2](#)). Namely, the live, metabolically active, and MHC-I<sup>+</sup> cells were sorted into either CD45<sup>+</sup> CD31<sup>−</sup> immune cells, CD45<sup>−</sup> CD31<sup>+</sup> endothelium, or CD45<sup>−</sup> CD31<sup>−</sup> remaining mesenchymal cells. The sorted populations were mixed in a 1:1:1 ratio to enrich for leucocytes and resident mesenchymal cells and sequenced in two separate libraries. Of note, we were able to sort a significantly lower number of CD45<sup>−</sup> CD31<sup>−</sup> resident mesenchymal cells from 18-month-old hearts, compared to young controls. We performed

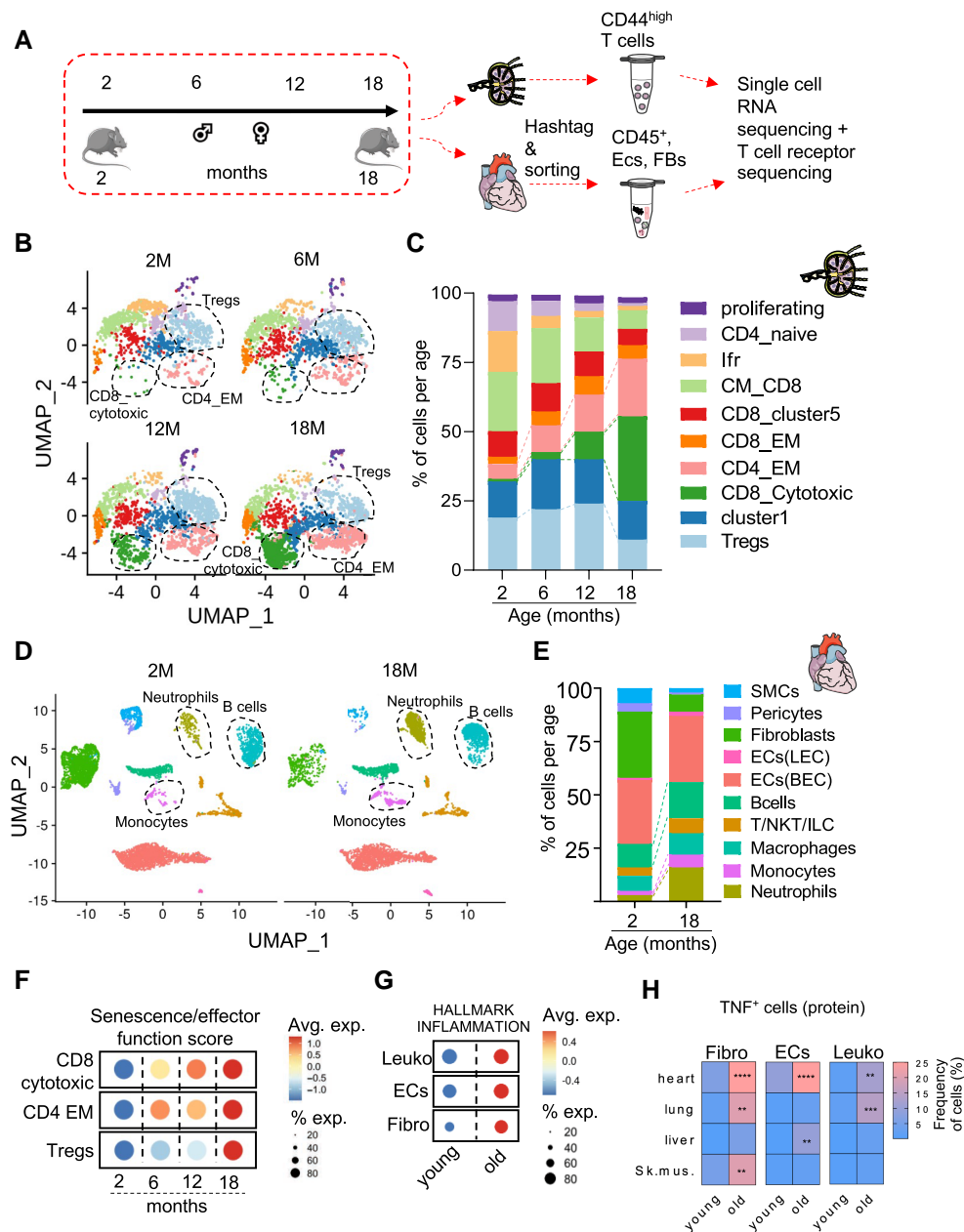


**Figure 1** Dissecting aging kinetics using single-cell transcriptomics from cardiac cells and T cells in heart-draining mediastinal lymph node simultaneously. Panel A: experimental outline for the sc-seq pipeline. Panel B: UMAP plot representation of the sorted 7243 mediastinal lymph node effector/memory T cells from 2-, 6-, 12-, to 18-month-old male and female C57BL/6J mice shown on a UMAP dimensionality reduction plot. Panel C: bar graph representation for the lymph node T cell subsets identified based on the Seurat clustering among the different age groups. Age groups were identified based on the hashtag antibody signal, which was demultiplexed prior to Seurat clustering. Panel D: UMAP plot representation of the sorted 12 613 non-cardiomyocyte cells from 2- (left) to 18- (right) month-old male and female hearts. Panel E: bar graph representation for the cardiac cell subset distribution among the 2- and 18-month-old hearts. Panel F: dot plot of the compiled scores for the average expression levels of gene sets ascribing a gene set of senescence and effector functions within mediastinal lymph node CD8-cytotoxic, CD4-EM, and Tregs among the different age groups. Size of the dot represents the percentage of cells expressing the gene set within each population and colour represents the expression level. Panel G: dot plot of the compiled score for genes related to the inflammaging process within cardiac fibroblasts, endothelial cells, and leucocytes from 2- to 18-month-old hearts. Each age group comprises four mice that were pooled into two meta-mice (one male and one female in each pool) for panels (B, C, D, E, F, G). Panel H: heatmap of the frequency of intracellular TNF<sup>+</sup> expression in fibroblasts, endothelial cells, and leucocytes, assessed by flow cytometry in different anatomical sites in 2- and 18-month-old female C57BL/6J mice (n = 6). Statistical test: two-way ANOVA followed by Sidak's multiple comparisons test. \*\**P* < 0.01, \*\*\**P* < 0.001, \*\*\*\**P* < 0.0001.

canonical correlation analysis for batch correction of the data from 2- to 18-month-old cardiac cells.<sup>19</sup>

After filtering out cells with low RNA content, doublets, and minor contaminating cell subsets, we defined 7243 T cells from the different age groups from the mediastinal lymph nodes, and 12 613 non-cardiomyocyte cells from 2- to 18-month-old hearts. Cardiomyocytes were not purified as they exceed the size limits of the droplet-based sc-seq technology used in this study. Clustering analysis of the gene expression data from the lymph node T cells yielded 10 clusters (Figure 1B, see [Supplementary material online, Figure S4A, Supplementary material online, Table S5](#)). The clusters defined included central memory (*Cd8a*, *Sell*, *Ccr7*, and *Cd44*) and effector memory (*Cd8a*, *Cx3cr1*, *Cd127*, and *Cd44*) CD8 T cells, cytotoxic (*Cd8a*, *Ngk7*, *Gzmk*, and *Cd5*) CD8 T cells, effector memory (*Cd4* and *Cd44*), and T regulatory (*Cd4* and *Foxp3*) CD4 T cells. We also observed a small subset of naive CD4 T cells (*Ccr7*, *Lef1*, *Dapl1*, and *Satb1*), which were likely remnants from the cell sorting strategy, and a subset exhibiting an interferon-responsive gene signature (e.g.: *lfit3*, *lfit3b*, *lfit1*, *lfit2*, *lrf7*, and *lsg15*, termed *lfr* subset). Additionally, two clusters (cluster 1 and CD8 cluster 5) could not be defined based on the classical markers of T cell subsets, expressed genes associated with damaged cells in sc-seq data (*Malat1*, *Lars2*, *Gm42418*, and *Gm2682*), presumably induced by the tissue dissociation protocol, and had low counts of productive TCR sequences assigned per cell base. These two clusters were thus removed from downstream analysis.

A linear decline in CD4 naive, *lfr* cluster, and CD8 central memory T cells was observed with aging, with a contrasting linear increase in CD4 effector memory and CD8 cytotoxic T cell abundance. Strikingly, T regulatory cells dropped in numbers from the 12 to 18 months age groups (Figure 1B, C). Clustering of the 2- and 18-month-old cardiac non-myocyte yielded 10 subsets (Figure 1D, see [Supplementary material online, Figure S4B, Supplementary material online, Table S5](#)) including blood vascular (BEC) and lymphatic (LEC) endothelial cells, fibroblasts, macrophages, neutrophils, B cells, monocytes, smooth muscle cells, pericytes, and a cluster comprising T cells, NKT cells, and ILC2 (T/NKT/ILC). Within the cardiac leucocyte populations (Figure 1D and E), neutrophils were more abundant in the 18-month-old hearts. B cells and monocytes were also more abundant though to a lesser extent.

Based on a compiled score assigned to mediastinal lymph node T cells per cell base for 'effector functions and cellular senescence' gene signatures, we observed a linear increase in the score within CD4 effector memory T cells (CD4\_EM), and in CD8 cytotoxic T cells (CD8\_cytotoxic) along the aging axis. These scores were mainly driven by the transcripts *Cxcr3*, *Rela*, *Ccl5*, *Tigit*, and *Pdcd1* (see [Supplementary material online, Figure S6](#)). On the other hand, T regulatory cells (Tregs) showed an abrupt increase in the 'effector functions and cellular senescence' score gene signature from the 12- to 18-month age groups (Figure 1F, see [Supplementary material online, Table S3, Supplementary material online, Figure S6](#)). The up-regulated expression levels of several pro-inflammatory transcripts in 18-month-old Tregs indicated that these cells might exhibit an unstable phenotype and acquire inflammatory functions with aging.<sup>20</sup>

Next, we identified the sex of the cells based on the expression of *Xist* gene in female cells and *Ddx3y*, *Eif2s3y*, *Gm29650*, *Kdm5d*, and *Uty* gene in male cells. Based on the gene definition, 33% of the cells were defined as female cells, 16% as male cells, and 51% of the lymph node cells could not be ascribed to a defined sex (see [Supplementary material online, Figure S7A](#)). Pro-inflammatory and T helper-1 response (*Cxcr3*, *Stat1*, *Ctla2a*, *Nfkb2*, and *S100a6*), cytokine (*Gzmk*), and exhaustion (*Lag3*, *Pdcd1*, *Tigit*, and *Tox2*) genes were up-regulated in 18-month-old compared to 2-month-old T cells, in both male and female T cells (see [Supplementary material online, Figure S7B, Supplementary material online, Table S5](#)).

Additionally, we observed an increased score of the gene set *hallmark inflammation* in all main cardiac subsets from 2 to 18 months (Figure 1G, see [Supplementary material online, Table S3](#)). Flow cytometry analysis further confirmed these findings by showing an increased cardiac influx of neutrophils and MHC-II<sup>+</sup> CCR2<sup>+</sup> monocyte-derived macrophages (see [Supplementary material online, Figure S5A and B](#)). We also observed increased production of TNF by immune cells (CD45<sup>+</sup>), fibroblasts (CD45<sup>-</sup> CD31<sup>-</sup>), and endothelial cells (CD45<sup>-</sup>CD31<sup>+</sup>) purified from the aged myocardium (Figure 1H, see

[Supplementary material online, Figure S8A](#)). Though this age-dependent TNF increase was observed in other organs (lung and liver), it was more pronounced in the heart (Figure 1H). Moreover, we observed an age-related reduction in the expression of the immune checkpoint inhibitor PD-1 in myocardial endothelial cells, but not in other organs (see [Supplementary material online, Figure S8B and C](#)). Using the same genes for sex definition in the heart yielded a more homogenous clustering pattern between male and female cells (see [Supplementary material online, Figure S9A](#)). Globally, pro-inflammatory genes such as *Il1b*, *S100a9*, *Ccl5*, and *Cd6* were up-regulated both in male and female 18-month-old cardiac cell subsets compared to 2-month-old cells (see [Supplementary material online, Figure S9B](#)). Interestingly, the alarmin *S100a8/9* was consistently up-regulated in cardiac immune cell subsets and also in endothelial cells and fibroblasts (see [Supplementary material online, Figure S9C, Supplementary material online, Table S5](#)), which has been indicated as a predictor of increased cardiovascular risk.<sup>21</sup>

### 3.2 Aberrantly expanded, effector-like and IFN- $\gamma$ producing T cells build up in the aged heart-draining lymph nodes

Reduction in the diversity of the T cell repertoire is a major feature of physiological aging.<sup>6</sup> Thus, we next analysed the clonal expansion status of individual T cell clones in the different subsets along the aging axis (Figure 2A). The TCR variable region sequences of each individual T cell were combined with their respective gene expression data, and each TCR clonal expansion was calculated across the entire dataset. Interestingly, T cell clonal expansion was observed in the aged healthy mice. T cell clonal expansion was mainly visible in the 18-month-old CD8\_cytotoxic cluster and to a lesser extent in the 18-month-old CD4\_EM and Treg clusters (Figure 2A).

Senescence and exhaustion of T cells with aging is a well-documented phenomenon.<sup>22</sup> However, the kinetics of aging within the different T cell sub-populations is not fully understood. We analysed gene sets associated with Th1/17 response, cytotoxicity, exhaustion, cellular senescence, and metabolic shifts towards glycolytic processes (which promotes the expansion of inflammatory T cells<sup>23</sup>), and compiled a score for the average gene expression of each gene set within different subsets. Interestingly, immediately (6–20 clones) and highly expanded (>20 clones) groups up-regulated gene signatures associated with Th1/17 response, cytotoxicity, cellular senescence, exhaustion, and glycolytic activity. (Figure 2B, see [Supplementary material online, Table S3](#)). Particularly, an IFN- $\gamma$  production signature built up in the aged CD8 cytotoxic, CD4 EM, and in the Treg clusters (Figure 2C, see [Supplementary material online, Table S3](#)). This was indicated by a higher expression of *Tbx21* (T-bet), *Eomes*, *Cxcr3*, and *Itgb1* (which encodes for CD29, surface surrogate marker for IFN- $\gamma$  producing T cells<sup>24</sup>) in the 12- and 18-month-old cells (Figure 2D). IL4 and IL13 production signature was down-regulated in the 18-month-old cells (see [Supplementary material online, Figure S1S0A and B, Supplementary material online, Table S3](#)), suggesting a particular relevance for IFN- $\gamma$  signaling in aging mechanisms. Interestingly, the IFN- $\gamma$  production signature overlapped with the increase in clonal expansion, with 18-month-old cytotoxic T cells showing the highest overlap between the two signatures (Figure 2E). By flow cytometry, we confirmed that an IFN- $\gamma$ <sup>+</sup> CD29<sup>+</sup> population was expanding along the aging axis in both CD4 and CD8 T cells (Figure 2F). This CD29<sup>+</sup> T cell population was found to be increased in other lymphoid sites during aging such as the mesenteric lymph node, spleen and in blood, and to a lesser extent in the popliteal lymph node, which drains the hind limb skeletal muscle and skin (Figure 2G).

### 3.3 An IFN- $\gamma$ response signature in the myocardium is potentially fuelled by aged T cells

We next wanted to address how the aged T cell compartment influences the inflammaging status of older hearts. First, we focused on the T cells infiltrating the myocardium. Cardiac-infiltrating T cells from 18-month-old



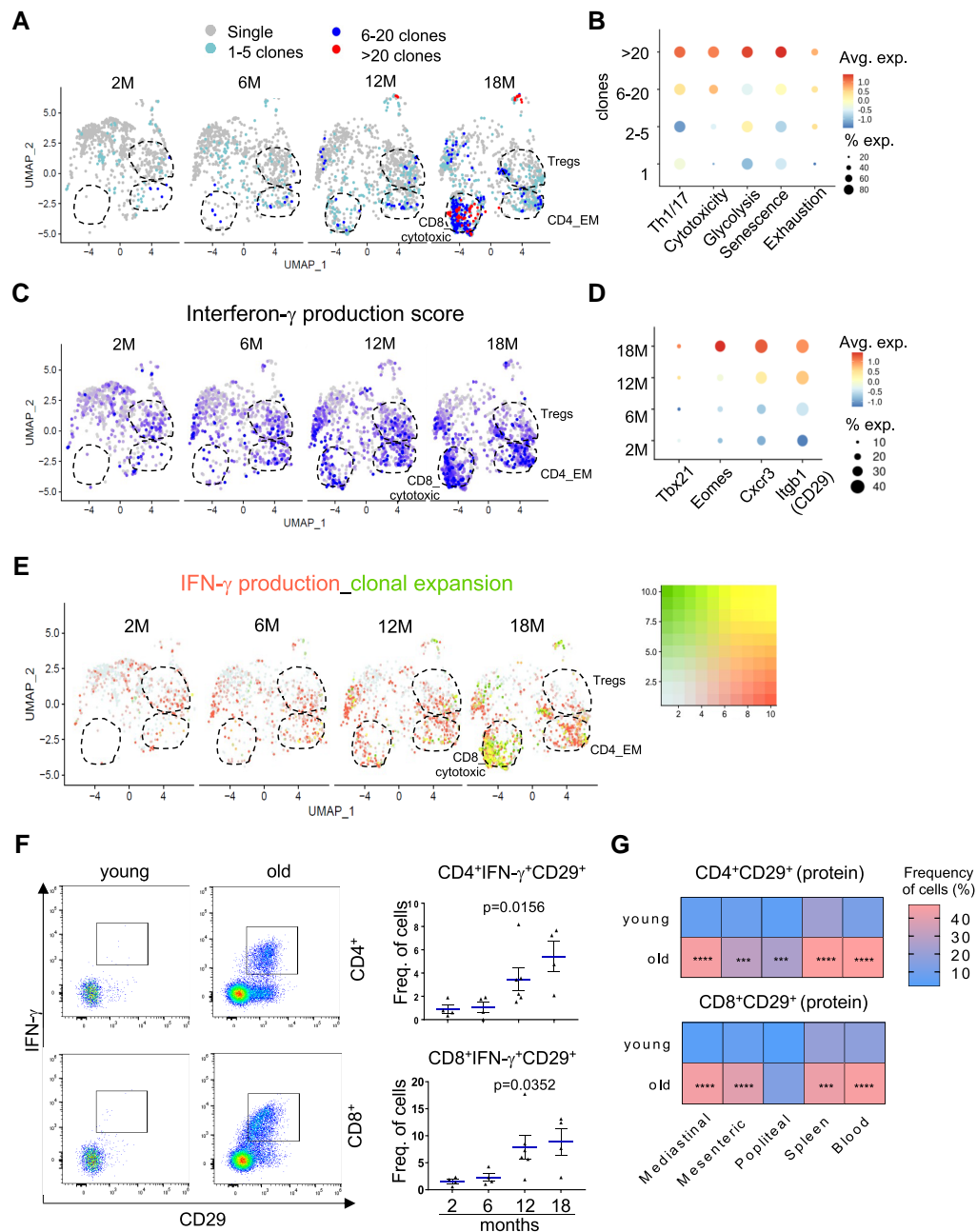


**Figure 2** A clonally expanded, effector and IFN- $\gamma$  producing profile of T cells in mediastinal lymph node T cells from aged mice. Panel A: T cell receptor sequencing analysis overlaid on UMAP plots of the T cell subsets from the different age groups. Cells are colour-coded according to how many times the T cell receptor is repeated i.e. clonal size. The identity of the T cell receptor clones is based on the variable chain usage (VDJ) gene segments and the CDR3 sequences. Panel B: dot plot of the compiled score for gene sets ascribed to Th1/17 effector, cytotoxicity functions, glycolysis activity, cellular senescence-related genes, and exhaustion classified based on the definition of the clonally expanding class. Panel C: feature plot for the expression score of IFN- $\gamma$  production gene set in each cell projected onto dimension reduction 'UMAP' plots to identify the signature expression in the different age groups in lymph node T cells. Panel D: dot plot of the averaged expression of *Tbx21*, *Eomes*, *Cxcr3*, and *Itgb1* within CD4-EM, Tregs, and CD8 cytotoxic T cells along the aging axis. Panel E: feature plot showing the overlapping expression score of IFN- $\gamma$  production gene set (red) and clonal expansion (green) per cell base in the lymph node T cell subsets. Cells with a high overlapping score are indicated with a yellow colour. Each age group comprises four mice that were pooled into two meta-mice (one male and one female in each pool) for panels (A, B, C, D, E). Panel F: (left) representative flow cytometry plot from young (2 months old) and old (18 months old) mediastinal lymph node for CD29 (*Itgb1*) and IFN- $\gamma$  double positive population in CD8 and CD4 T cells from mediastinal lymph nodes. (Right) frequency of CD4<sup>+</sup> IFN- $\gamma$ <sup>+</sup> CD29<sup>+</sup> (left) and CD8<sup>+</sup> IFN- $\gamma$ <sup>+</sup> CD29<sup>+</sup> (right) T cells from mediastinal lymph nodes of 2-, 6-, 12-, and 18-month-old C57BL/6J mice. The bar graphs indicate the group mean values  $\pm$  SEM per group ( $n = 4-6$ ), and the distribution of each individual value. Statistical test: ordinary one-way ANOVA followed by Dunnett's multiple comparison test. Panel G: heatmap depicting the frequency of CD29<sup>+</sup> CD4<sup>+</sup> (upper panel) and CD8<sup>+</sup> (lower panel) T cells assessed by flow cytometry in different anatomical sites in 2- and 18-month-old female C57BL/6J mice ( $n = 6$ ). Statistical test: two-way ANOVA followed by Sidak's multiple comparisons test. \*\*\* $P < 0.001$ , \*\*\*\* $P < 0.0001$ .

mice presented a higher IFN- $\gamma$  production gene signature (Figure 3A) and up-regulated effector molecules such as *Gzmb* and *Prf1* (see [Supplementary material online, Figure S9D](#)). Moreover, we confirmed by flow cytometry an increased frequency of myocardial CD29<sup>+</sup> T cells, which associated with increased IFN- $\gamma$  production (Figure 3B, see [Supplementary material online, Figure S10E](#)). The frequency of CD29<sup>+</sup> was also increased in T cells purified from aged lungs and livers, suggesting a systemic IFN- $\gamma$  production bias along the aging process (see [Supplementary material online, Figure S10F](#)). To analyse the global immunological changes affecting the heart, we made use of publicly available cardiac bulk RNA sequencing data from the *Tabula Muris Senis* consortium.<sup>25</sup> Gene set enrichment analysis (GSEA) was performed on a kinetic from 3- to 27-month-old cardiac tissue of C57BL/6J mice using Pearson's correlation. Pathways related to inflammatory response, IFN- $\gamma$  response, and IFN- $\gamma$  production positively correlated with the aging trajectory (Figure 3C). In contrast, IL-4 signaling pathway was not up-regulated in the myocardium (see [Supplementary material online, Figure S10C and D, Supplementary material online, Table S3](#)). Interestingly, the normalized score of the IFN- $\gamma$  response gene set was increasingly up-regulated starting from 18 months of age, which matches the Treg senescence breaking-point observed in the lymph node T cells. We next performed a meta-analysis from 2- to 18-month-heart single-cell RNA-seq data from the *Tabula Muris Senis*, our in-house generated data from Figure 1D, and single-nucleus RNA seq data<sup>26</sup> from the same age groups (Figure 3D) to pinpoint the subsets mainly affected by the IFN- $\gamma$  signalling. All three datasets were integrated and corrected for batch effects using the Seurat package. The data generated from our lab were pre-enriched for the less abundant cardiac leucocytic populations (CD45<sup>+</sup> CD31<sup>-</sup>), while the data from the *Tabula Muris Senis* and from Vidal *et al.* included cardiomyocytes, which were sequenced through SMART-seq and single-nuclei-seq platforms, respectively. This approach allowed for a better depth and more robustness when analysing the different cardiac cell subsets.

Genes downstream to IFN- $\gamma$  signaling were up-regulated in 18-month-old compared to 2-month-old heart cells. This included *Irf1*, *Irf9*, *Jak1*, *Stat1*, *Smad7*, and the two immunoproteasome components *Psmb8* and *Psmb9*, which are induced by IFN- $\gamma$  (Figure 3E). Additionally, the IFN- $\gamma$  response gene set score was higher for cardiomyocytes, fibroblasts, endothelial cells, and leucocytes from 18-month-old mice (Figure 3F).

So far, our data point towards an accumulated senescence and exhaustion profile of the T cell compartment in the heart-draining lymph node, which aligns with an inflammatory burden that builds up in cardiac tissue and an increased IFN- $\gamma$  response signature. We thus wanted to better characterize the potential impact that the senescent T cells impart on the myocardial cell subpopulations. We used NicheNet,<sup>27</sup> an algorithm that probes for ligand-receptor interacting partners together with downstream signaling targets that are being affected in the recipient cells. CD4<sub>EM</sub>, Tregs, and CD8<sub>cytotoxic</sub> T cells were used as the ligand source and, the different cardiac subsets were probed for target gene perturbations in the 18-month compared to the 2-month-old cells. Interestingly, NicheNet inferred connections between Hmgb1 (a secreted inflammatory mediator in response to IFN- $\gamma$ ,<sup>28</sup>) Itgb1 or CD29 from the T cell subsets, and pro-inflammatory responder genes in cardiac macrophages, fibroblasts, and endothelial cells (see [Supplementary material online, Figure S11](#)). Gene ontology analysis of the top target genes interacting with the aged T cells indicated a positive regulation of response to cytokines and inflammatory signatures in cardiac cell subsets (see [Supplementary material online, Figure S11](#)).

### 3.4 Shifts in the metabolic profile of aging T cells correlate with their effector state

Activation of T cells has been correlated with an increased utilization of the glycolytic pathway for energy production, which is required as a fast energy source for these activated T cells to proliferate and produce effector molecules.<sup>29,30</sup> In order to track whether such metabolic shifts are observed in the aging mediastinal lymph node T cells, we made use of compiled gene

scores for oxidative phosphorylation (OxPhos), fatty acid oxidation (FAO), and glycolysis for T cells across the different age groups. Interestingly, we observed a linear increase in glycolysis and fatty acid oxidation gene set scores, and a mild decrease in OxPhos score along the aging axis (see [Supplementary material online, Figure S12A and B, Supplementary material online, Table S3](#)). Fatty acid oxidation is a key pathway required for the generation of memory CD8 T cells.<sup>31</sup> T cells with an increased glycolytic score also showed an overlap with a high score for IFN- $\gamma$  response (see [Supplementary material online, Figure S12C](#)), further supporting the notion that metabolic shifts in the mediastinal lymph node T cells go in parallel with their pro-inflammatory state.

### 3.5 Myocardial IFN- $\gamma$ response is intertwined with metabolic shifts resembling heart failure

IFN- $\gamma$  is a pleiotropic cytokine, which is involved in regulating immune reactions in ischaemic and non-ischaemic cardiomyopathies, and in promoting a pro-fibrotic response.<sup>32–34</sup> It has also been associated with insulin resistance and shifts of glycaemic control in skeletal muscles.<sup>35</sup> Thus, we hypothesized that an increased IFN- $\gamma$  response signature can potentially correlate with metabolic shifts in the heart. Focusing on cardiomyocytes from the *Tabula Muris Senis* dataset, we compiled gene scores for OxPhos, fatty acid oxidation, and glycolysis from young (3 months old) and aged (18, 21, and 24 months old) cardiomyocytes. The gene set scores showed metabolic shifts compatible with the shifts seen in failing hearts,<sup>36</sup> which is presented by a reduction in OxPhos, FAO scores, and a higher glycolysis score (Figure 4A, see [Supplementary material online, Figure S153](#)). In aged non-cardiomyocyte subsets from our own data, OxPhos was consistently down-regulated (Figure 4B). Down-regulation of the OxPhos signature overlapped with an increase in IFN- $\gamma$  response in old cardiomyocytes (Figure 4C). Using GSEA of OxPhos, FAO, and glycolysis on the generated bulk RNA-seq data from 3- to 27-month-old cardiac tissues from the *Tabula Muris Senis* indicated down-regulation of all three metabolic pathways along the whole aging time course (Figure 4D). Interestingly, the down-regulation of metabolic pathways was more pronounced in bulk mRNA sequencing data from cardiac tissue compared to liver and skeletal muscle (see [Supplementary material online, Figure S14B and C](#)). Lung and spleen on the other hand did not show such down-regulation (see [Supplementary material online, Figure S14A and D](#)) potentially indicating an organ specific modulation of metabolic pathways along the aging axis.

### 3.6 IFN- $\gamma$ stimulation of iPSC-derived cardiomyocytes recapitulates the metabolic shifts seen in aging

To address the direct effect of prolonged exposure to IFN- $\gamma$  stimulation on cardiomyocytes, we made use of human cardiomyocytes derived from iPSCs (iPSCs-CM). Five-week-old iPSCs-CM were stimulated with recombinant IFN- $\gamma$  (10 IU/mL) for 1 week or 4 weeks (Figure 5A). IFN- $\gamma$  stimulation did not affect the morphology of the cells (Figure 5B), nor did it affect the mitochondrial network structure (Figure 5C). This underscores that the chronic IFN- $\gamma$  treatment had no direct toxic effects on the mitochondrial and cell morphology in iPSC-CM. One week after IFN- $\gamma$  stimulation, the oxygen consumption rate (OCR) and extracellular acidification rate (ECAR) were measured by a Seahorse XF assay. ECAR, which is a measurement of glycolytic activity, was reduced compared to control cultures, while OCR, a measurement of OxPhos activity, was not affected. Four weeks after IFN- $\gamma$  stimulation, the effects were more pronounced, and both OCR and ECAR were significantly reduced compared to control cultures (Figure 5D). Taken together, these findings show that chronic IFN- $\gamma$  stimulation mediates metabolic changes in cardiomyocytes compatible with the transcriptomic profile observed in aging myocardial cells, as well as in failing hearts.<sup>36</sup>

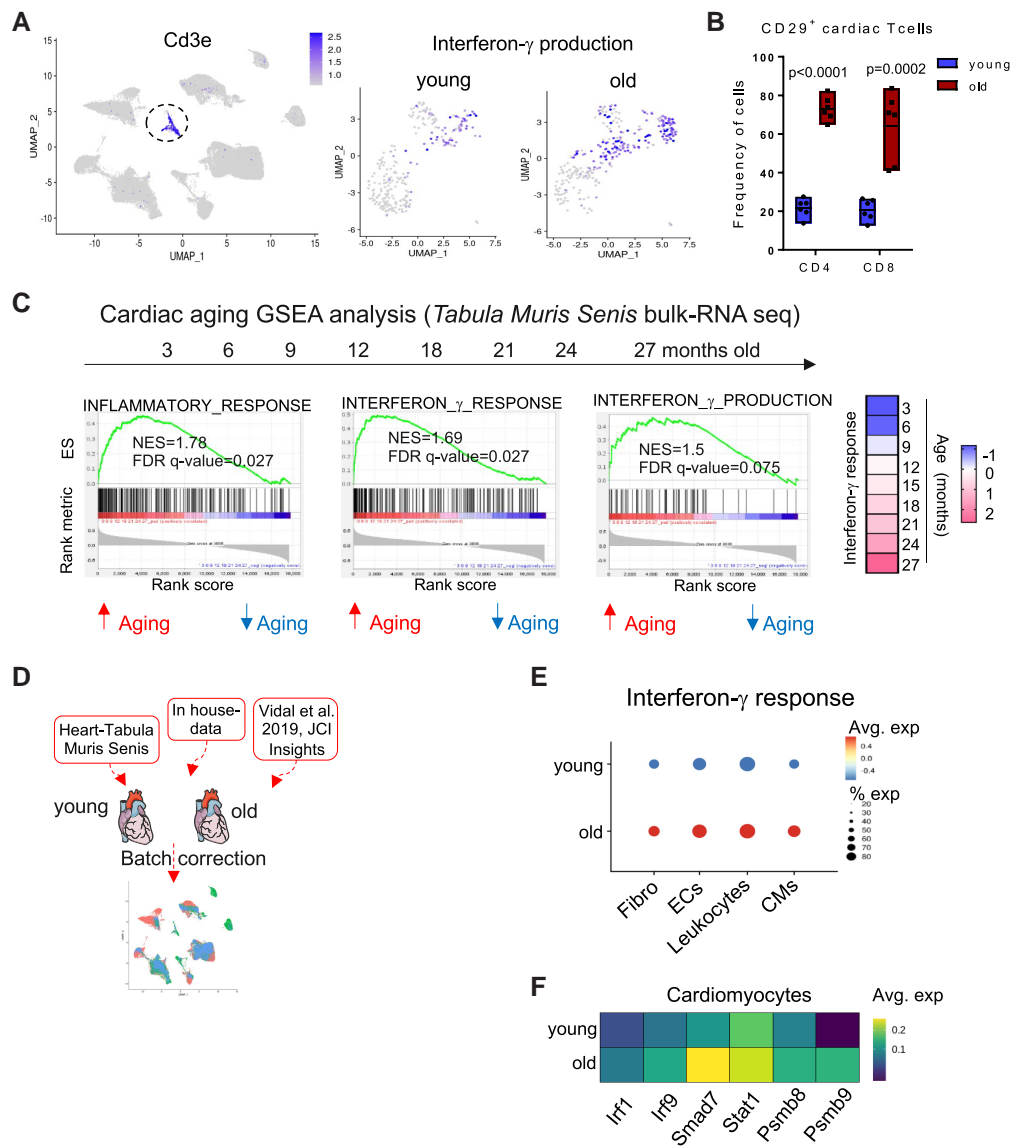


**Figure 3** An IFN- $\gamma$  signature builds up in aged hearts. Panel A: (left) feature plot of Cd3e indicating T cells within the heart sc-seq dataset. (Right) Feature plot for the expression score of interferon- $\gamma$  production gene set within the cardiac T cells in 2- and 18-month-old hearts after subsetting and re-clustering. Panel B: frequency of CD29<sup>+</sup> CD4<sup>+</sup> and CD8<sup>+</sup> T cells from heart tissue of 2- and 18-month-old female C57BL/6J mice. The bar graphs indicate the group mean values  $\pm$  SEM per group ( $n = 6$ ), and the distribution of each individual value. Statistical test: unpaired  $t$ -test. Panel C: (left) gene set enrichment analysis of inflammatory response, IFN- $\gamma$  response, and IFN- $\gamma$  production genes in an age range of 3–27 months from cardiac tissue of C57BL/6J mice from the Tabula Muris Senis bulk RNA-seq data. Normalized enrichment score (NES) and false discovery rate (FDR) are indicated in the graphs. (Right) heatmap of the normalized score of IFN- $\gamma$  response gene set in cardiac tissue of the different ages. Blue indicates down-regulation and red indicates up-regulation of the signature. All replicates from the Tabula Muris Senis per age group were used for the analysis. An FDR value <0.25 was considered significant. Panel D: computational pipeline for integrating the cardiac single-cell sequencing datasets. Panel E: dot plot of the compiled score for IFN- $\gamma$  response gene set in cardiac fibroblasts, endothelial cells, macrophages, and cardiomyocytes (CMs) from 2- to 18-month-old hearts. Panel F: heatmaps of selected differentially expressed genes from the IFN- $\gamma$  response gene set in young and old cardiomyocytes from the Tabula Muris Senis data.<sup>25</sup> Each age group comprises four mice that were pooled into two meta-mice (one male and one female in each pool) for in-house generated sc-seq data.

## 4. Discussion

In the present study, we bring to focus the aging process as an important aspect that is often neglected in animal models when studying the role played by the immune system in cardiovascular pathologies. Using longitudinal single-cell RNA transcriptomics, we observed that effector T cells expanding in the aged heart-draining lymph nodes up-regulate signatures of cellular senescence and pro-inflammatory effector functions, marked by

a strong IFN- $\gamma$  production signature. Additionally, we report that an IFN- $\gamma$  responsive program amasses with age in all main myocardial cell subsets, contributing to local baseline inflammation and metabolic rewiring, recapitulating some important features of heart failure.

Our profiling of T cell subsets from the heart-draining mediastinal lymph node from aged mice showed increased pro-inflammatory gene expression on effector T cells such as *Ccl5*, *Rela*, *Batf*, *Stat1*, and *Cxcr3*, and an increase in exhaustion markers such as *Tox*, *Lag3*, and *Tigit*. Mogilenko et al.<sup>37</sup>

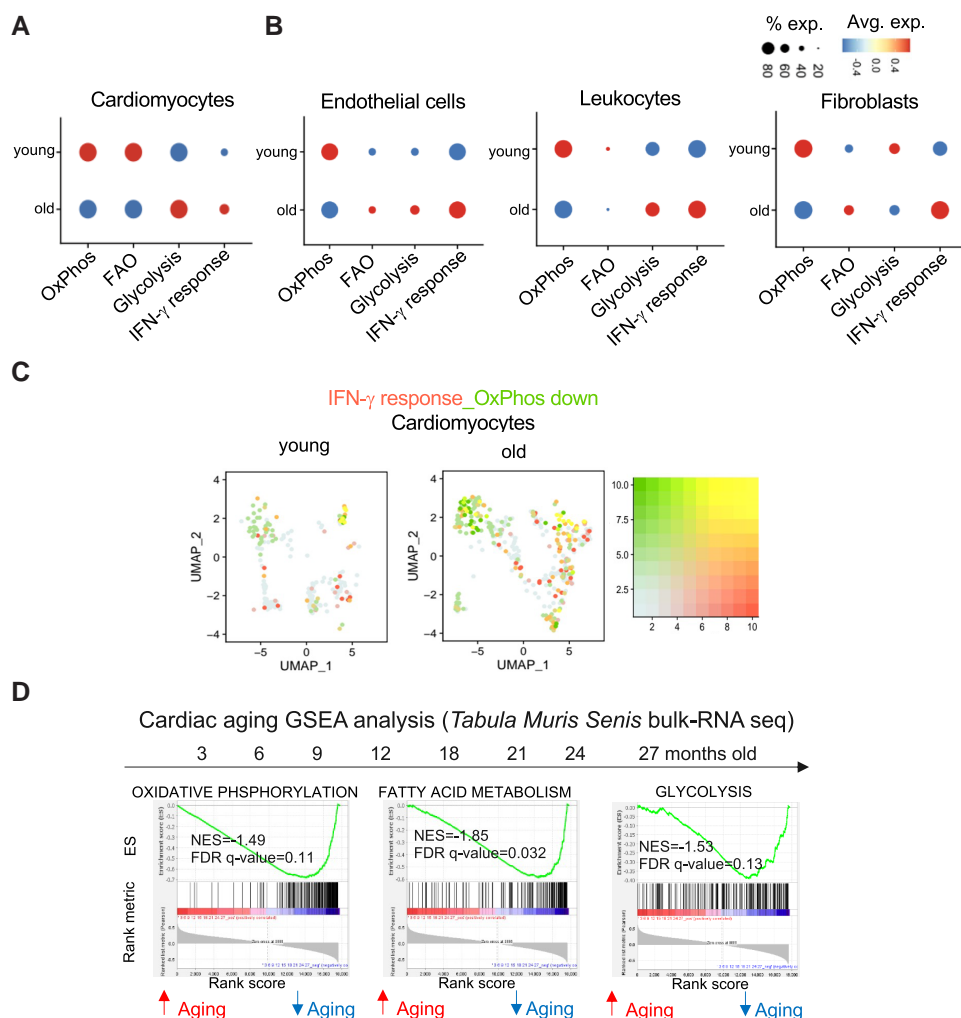


**Figure 4** Dynamics of interferon- $\gamma$  response and metabolic gene signatures in aged cardiomyocytes. Panel A: dot plot of the compiled score for OxPhos, FAO, glycolysis, and interferon- $\gamma$  response gene sets in young and old cardiomyocytes from the *Tabula Muris Senis* data.<sup>25</sup> Panel B: dot plot of the compiled score for OxPhos, FAO, glycolysis, and interferon- $\gamma$  response gene sets in young and old endothelial cells, leukocytes, and fibroblasts from in-house generated sc-seq data. Panel C: feature plot showing the overlapping expression score of IFN- $\gamma$  response gene set (red) and the expression score of down-regulation of OxPhos gene set (green) per cell base in young, and old cardiomyocytes. Cells with a high overlapping score are indicated with a yellow colour. Panel D: gene set enrichment analysis (GSEA) of Oxphos, FAO, glycolysis gene sets in an age range of 3–27 months from cardiac tissue of C57BL/6J mice from the *Tabula Muris Senis* bulk RNA-seq data. Normalized enrichment score (NES) and false discovery rate (FDR) are indicated in the graphs. All replicates from the *Tabula Muris Senis* per age group were used for the analysis. An FDR value <0.25 was considered significant. Each age group comprises four mice that were pooled into two meta-mice (one male and one female in each pool) for in-house generated sc-seq data.

reported a unique *Gzmk*<sup>+</sup> aging associated CD8 T cell subset found in spleen and in different non-lymphoid tissues, which showed high T cell clonal expansion. We found a similar subset of CD8 T cells in the aged mediastinal lymph node. Interestingly, we found no shared TCRs between both datasets. This potentially implies that the expanding clones in our dataset might respond to cardiac-specific antigens or preferentially reside in cardiac tissue, though this remains to be tested. We additionally profiled the activated CD44<sup>high</sup> Tregs and showed that they rapidly decline after 12 months and gain a pro-inflammatory profile based on up-regulation of genes such as *Stat1*, *Cxcr3*, and *Ccl5*. Taken together, we propose from these shifts that physiological aging of the mediastinal lymph node T cell compartment starts from an overly activated effector T cell compartment, which may eventually be sufficient to break Treg control.

We and others have previously reported increased inflammatory mediators, and pro-fibrotic and cellular senescence genes in the aging

heart.<sup>12,26,38</sup> In our dataset, we observed several cell specific genes that were regulated in the aged myocardium supporting such a notion. For example, fibroblasts showed up-regulated pro-fibrotic genes and anti-angiogenic genes such as *Efemp1*,<sup>39</sup> *Cebpb*,<sup>40</sup> and *Serpina3n*.<sup>41</sup> Endothelial cells revealed up-regulated senescence genes (*Cdkn1a*<sup>42</sup> and *Adamts1*<sup>43</sup>) and down-regulated angiogenesis genes (*Aplnr*<sup>44</sup>). Smooth muscle cells had up-regulated *Mt1*, a gene involved in pathological vessel remodelling.<sup>45</sup> Several inflammatory mediators were up-regulated by most immune cell subsets including *Il1b*, *Ccl6*, and *Ccl6*. Interestingly, the expression of the two alarmins *S100a8/a9* was not only limited to immune cells but was also up-regulated by fibroblasts and endothelial cells. These molecules have been associated with an increased risk of cardiovascular disease,<sup>21</sup> but their generalized expression in the aged myocardium needs further investigation. It is of crucial importance to understand the immuno-metabolic crosstalk in the heart to face the current challenges in



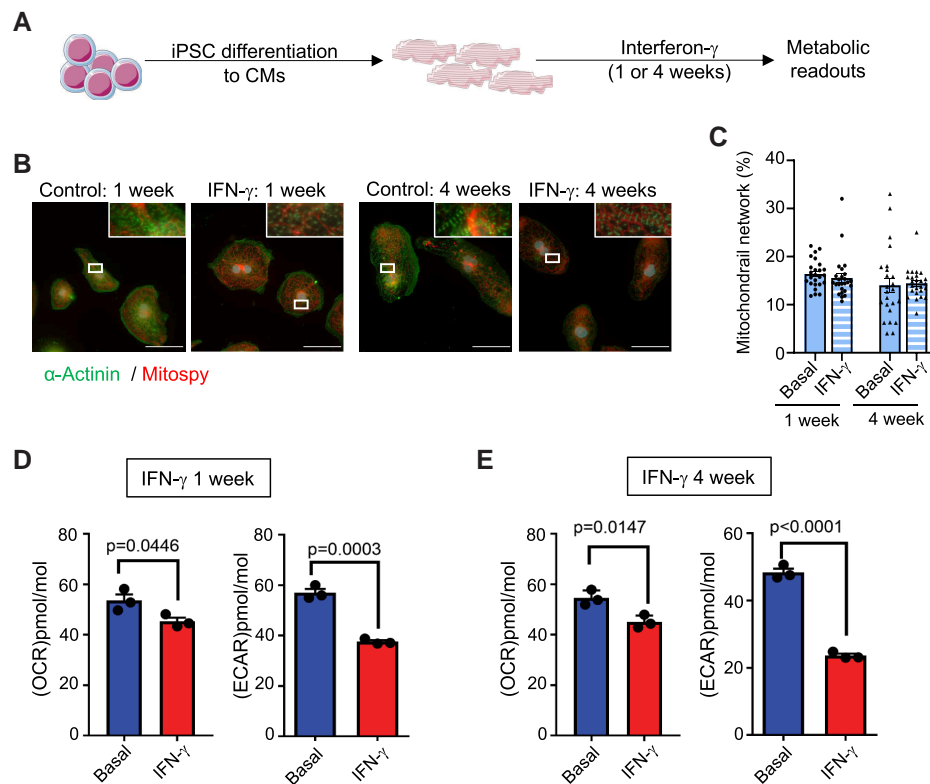


**Figure 5** Effect of IFN- $\gamma$  stimulation on iPSC derived cardiomyocytes. Panel A: schematic representation of the experiment outline. Panel B: visualization of sarcomeric ( $\alpha$ -actinin/green) and mitochondrial (Mitospy/red) structure of iPSC-CM with treatment of IFN- $\gamma$ . Scale bars = 50  $\mu$ m Panel C: quantification of mitochondrial network structures based on the Mitospy-staining. Statistical analysis was performed with Mann-Whitney. Every dot represents one analysed picture. Panels D and E: basal respiration (OCR) and H<sup>+</sup> production (ECAR) of iPSC-derived cardiomyocytes after 1 (D) or 4 (E) weeks of IFN- $\gamma$  stimulation or control cultures. Each point indicates group mean value  $\pm$  SEM per group ( $n = 3$  differentiations of five measurements each). Statistical test: unpaired  $t$ -test.

understanding cardiovascular disease.<sup>46</sup> Based on our observations from bulk and single-cell transcriptomic data, together with metabolic assays on iPSC-derived cardiomyocytes, we hypothesize that IFN- $\gamma$  from mediastinal lymph node T cells is required for shaping the inflammaging profile of the heart and is also contributing to the metabolic shifts, which happen with age.<sup>47</sup> Mice globally over-expressing IFN- $\gamma$  exhibit a high inflammatory response in multiple organs.<sup>48</sup> Also, constitutive expression of IFN- $\gamma$  in liver impairs cardiac function and induces LV dilation.<sup>49</sup> On the other hand, IFN- $\gamma^{-/-}$  mice were described to have improved glucose tolerance and increased physical activity.<sup>50</sup> Chronic inflammation has been associated with oxidative stress and mitochondrial dysfunction as seen in heart failure.<sup>51</sup> Interestingly, IFN- $\gamma$  has been associated with metabolic dysfunction seen in Chagas cardiomyopathy.<sup>52</sup>

Whereas we found a consistent age-related down-regulation of transcripts associated to OxPhos in all major myocardial cell subsets across different datasets, the impact of aging on the regulation of glycolytic pathways is less clear. Bulk RNA-seq data from the *Tabula Muris Senis* consortium indicated an overall down-regulation of transcripts related to the glycolytic pathway in the aged myocardium. On the other hand, changes in glycolysis from our generated and from the *Tabula Muris Senis* single-cell RNA-seq data were subset specific, and were up-regulated in aged cardiomyocytes, endothelial cells, and leucocytes. The latter hold important similarities to what is observed in TAC model, in which glycolysis-related transcripts were shown to be initially up-regulated but then down-regulated at chronic stages.<sup>53</sup> Whether these differences are related to the sequencing platform utilized remains to be addressed. In the functional cellular respiration assays, which we conducted using human iPSC-CM chronically incubated with low-dose IFN- $\gamma$ , a marked decrease in both OCR and ECAR was

observed, suggesting a reduction on oxygen consumption and glycolytic activity. Thus, our functional observations were more in line with the bulk mRNA findings from the *Tabula Muris Senis* consortium.

Chronic low-grade inflammation is a systemic hallmark of aging. In the present study, we indeed observed an overall increase in inflammatory mediators in several tissues, including heart, lung, liver, and skeletal muscle. Notwithstanding, we also observed some alterations that were particularly enriched in the aging myocardium. For instance, a heart-specific decrease in PD-L1 expression in myocardial endothelial cells suggests that the heart may be more susceptible to immune-mediated damage in elderly. Likewise, the expression levels of transcripts required for OxPhos were particularly down-regulated in aged hearts, but not in lungs and spleen.

Our study also has some important limitations. We acknowledge that our transcriptomic analyses and *in vitro* assays on cardiomyocytes do not provide final proof of the impact of IFN- $\gamma$  on the aging heart. We were able to confirm some of our findings at the protein level using flow cytometry. However, our analysis is not exhaustive, and post-transcriptional modifications still need to be further characterized in future studies. Moreover, the observations on the differential expression of transcripts related to the different metabolic pathways need to be carefully interpreted. Though we observed global shifts in mRNA levels that were consistent within each metabolic pathway, it is important to caution that cellular metabolism is regulated at the protein level,<sup>54</sup> and future functional studies using aged transgenic animals are necessary to understand the dynamics in the highly complex *in vivo* context.

Though unlikely to be the sole player, we propose that the IFN- $\gamma$  axis between T cells and the aging myocardium may be an important factor promoting myocardial immune-metabolic shifts typically seen in the failing

heart. Although physiological aging is not a disease entity per se, these mechanisms may help explain how age is associated with an increased risk of heart failure.

## Supplementary material

Supplementary material is available at *Cardiovascular Research* online.

## Authors' contributions

D.A., S.R., J.D., and G.C.R. conducted experiments and analysed data (FACS, cell sorting, microscopy, iPSC-CM generation, and respiration measurement). P.A. and A.E.S. conducted the single-cell RNA sequencing experiments. D.E.A. and G.C.R. analysed the single-cell RNA sequencing data. D.A., J.D., R.S., U.H., S.F., C.C., K.S.S., and GCR made substantial contributions to the conception and design of the present work. All co-authors contributed to the manuscript preparation.

## Acknowledgements

We thank Elena Vogel and Lisa Popiolkowski for the skilful technical assistance.

**Conflict of interest:** None declared.

## Funding

This work was supported by the German Research Foundation (DFG grant 411619907 to G.C.R. and 471241922 to KSB) and the European Research Area Network—Cardiovascular Diseases (ERANET-CVD JCT2018, AIR-MI Consortium grants 01KL1902 to G.C.R.). G.C.R. and C.C. were supported by the Interdisciplinary Centre for Clinical Research Würzburg (E-354 to G.C.R., E-353 to C.C.). G.C.R., C.C., E.A.S., U.H., J.D. and S.F. lead projects integrated in the Collaborative Research Centre 'Cardio-Immune interfaces', funded by the German Research foundation (SFB1525 grant number 453989101). R.S. was supported by a Humboldt Research Award from the Alexander von Humboldt Foundation and by the Canadian Institutes for Health Research (Foundation grant award 143299). This work was supported by the Core Unit Systems Medicine and by the Interdisciplinary Center for Clinical Research of the University Hospital Würzburg grant IZKF-Z6.

## Data availability

The raw and processed single-cell RNA-sequencing data presented in this study has been deposited in the NCBI Gene Expression Omnibus (GEO) database under the accession number GSE217098.

## References

- Coats AJS. Ageing, demographics, and heart failure. *Eur Heart J Suppl* 2019;**21**:L4–L7.
- Swirski FK, Nahrendorf M. Cardioimmunology: the immune system in cardiac homeostasis and disease. *Nat Rev Immunol* 2018;**18**:733–744.
- Franceschi C, Bonafè M, Valensin S, Olivieri F, De Luca M, Ottaviani E, De Benedictis G. Inflamm-aging. An evolutionary perspective on immunosenescence. *Ann N Y Acad Sci* 2000;**908**:244–254.
- Bollini S, Guzik TJ. Old, but gold? Not the case for the immune system when promoting systemic ageing. *Cardiovasc Res* 2022;**118**:e14–e16.
- Min H, Montecino-Rodriguez E, Dorshkind K. Reduction in the developmental potential of intrathymic T cell progenitors with age. *J Immunol* 2004;**173**:245–250.
- Britanova OV, Putintseva EV, Shugay M, Merzlyak EM, Turchaninova MA, Staroverov DB, Bolotin DA, Lukyanov S, Bogdanova EA, Mamedov IZ, Lebedev YB, Chudakov DM. Age-related decrease in TCR repertoire diversity measured with deep and normalized sequence profiling. *J Immunol* 2014;**192**:2689–2698.
- Jaiswal S, Natarajan P, Silver AJ, Gibson CJ, Bick AG, Shvartz E, McConkey M, Gupta N, Gabriel S, Ardissino D, Baber U, Mehran R, Fuster V, Danesh J, Frossard P, Saleheen D, Melander O, Sukhova GK, Neuberg D, Libby P, Kathiresan S, Ebert BL. Clonal hematopoiesis and risk of atherosclerotic cardiovascular disease. *N Engl J Med* 2017;**377**:111–121.
- Yager EJ, Ahmed M, Lanzer K, Randall TD, Woodland DL, Blackman MA. Age-associated decline in T cell repertoire diversity leads to holes in the repertoire and impaired immunity to influenza virus. *J Exp Med* 2008;**205**:711–723.
- Haynes L, Swain SL. Why aging T cells fail: implications for vaccination. *Immunity* 2006;**24**:663–666.
- Brubaker AL, Rendon JL, Ramirez L, Choudhry MA, Kovacs EJ. Reduced neutrophil chemotaxis and infiltration contributes to delayed resolution of cutaneous wound infection with advanced age. *J Immunol* 2013;**190**:1746–1757.
- Bujak M, Kweon HJ, Chatila K, Li N, Taffet G, Frangogiannis NG. Aging-related defects are associated with adverse cardiac remodeling in a mouse model of reperfused myocardial infarction. *J Am Coll Cardiol* 2008;**51**:1384–1392.
- Ramos GC, van den Berg A, Nunes-Silva V, Weirather J, Peters L, Burkard M, Friedrich M, Pinnecker J, Abeßer M, Heinze KG, Schuh K, Beyersdorf N, Kerkau T, Demengeot J, Frantz S, Hofmann U. Myocardial aging as a T cell-mediated phenomenon. *Proc Natl Acad Sci U S A* 2017;**114**:E2420–E2429.
- Alpert A, Pickman Y, Leipold M, Rosenberg-Hasson Y, Ji X, Gaujoux R, Rabani H, Starosvetsky E, Kveler K, Schaffert S, Furman D, Caspi O, Rosenschein U, Khatir P, Dekker CL, Maecker HT, Davis MM, Shen-Orr SS. A clinically meaningful metric of immune age derived from high-dimensional longitudinal monitoring. *Nat Med* 2019;**25**:487–495.
- Sayed N, Huang Y, Nguyen A, Krejcirova-Rajaniemi Z, Grawe AP, Gao T, Tibshirani R, Hastie T, Alpert A, Cui L, Kuznetsova T, Rosenberg-Hasson Y, Ostan R, Monti D, Lehallier B, Shen-Orr SS, Maecker HT, Dekker CL, Wyss-Coray T, Franceschi C, Jojic V, Haddad F, Montoya JG, Wu JC, Davis MM, Furman D. An inflammatory aging clock (iAge) based on deep learning tracks multimorbidity, immunosenescence, frailty and cardiovascular aging. *Nat Aging* 2021;**1**:598–615.
- Spyridopoulos I, Martin-Ruiz C, Hilkens C, Yadegarfar ME, Isaacs J, Jagger C, Kirkwood T, von Zglinicki T. CMV seropositivity and T cell senescence predict increased cardiovascular mortality in octogenarians: results from the Newcastle 85+ study. *Aging Cell* 2016;**15**:389–392.
- Gage GJ, Kipke DR, Shain W. Whole animal perfusion fixation for rodents. *JoVE* 2012 Jul 30; (65):e3564.
- Golde WT, Gollobin P, Rodriguez LL. A rapid, simple, and humane method for submandibular bleeding of mice using a lancet. *Lab Anim* 2005;**34**:39–43.
- Borchert T, Hübscher D, Guessoum CI, Lam TD, Ghadri JR, Schellinger IN, Tiburcy M, Liaw NY, Li Y, Haas J, Sossalla S, Huber MA, Cyganek L, Jacobshagen C, Dressel R, Raaz U, Nikolaev VO, Guan K, Thiele H, Meder B, Wollnik B, Zimmermann WH, Lüscher TF, Hasenfuss G, Templin C, Streckfuss-Bömeke K. Catecholamine-dependent  $\beta$ -adrenergic signaling in a pluripotent stem cell model of Takotsubo cardiomyopathy. *J Am Coll Cardiol* 2017;**70**:975–991.
- Butler A, Hoffman P, Smibert P, Papalexi E, Satija R. Integrating single-cell transcriptomic data across different conditions, technologies, and species. *Nat Biotechnol* 2018;**36**:411–420.
- Pandayan P, Zhu J. Origin and functions of pro-inflammatory cytokine producing foxp3+ regulatory T cells. *Cytokine* 2015;**76**:13–24.
- Averill MM, Kerkhoff C, Bornfeldt KE. S100a8 and S100a9 in cardiovascular biology and disease. *Arterioscler Thromb Vasc Biol* 2012;**32**:223–229.
- Mittelbrunn M, Kroemer G. Hallmarks of T cell aging. *Nat Immunol* 2021;**22**:687–698.
- Xu K, Yin N, Peng M, Stamatides EG, Shyu A, Li P, Zhang X, Do MH, Wang Z, Capistrano KJ, Chou C, Levine AG, Rudensky AY, Li MO. Glycolysis fuels phosphoinositide 3-kinase signaling to bolster T cell immunity. *Science* 2021;**371**:405–410.
- Nicolet BP, Guislain A, van Alphen FJ, Gomez-Eerland R, Schumacher TNM, van den Biggelaar M, Wolters MC. CD29 identifies IFN- $\gamma$ -producing human CD8<sup>+</sup> T cells with an increased cytotoxic potential. *Proc Natl Acad Sci U S A* 2020;**117**:6686–6696.
- Tabula Muris Consortium. A single-cell transcriptomic atlas characterizes ageing tissues in the mouse. *Nature* 2020;**583**:590–595.
- Vidal R, Wagner JUG, Braeuning C, Fischer C, Patrick R, Tombor L, Muhly-Reinholz M, John D, Kliem M, Conrad T, Guimarães-Camboa N, Harvey R, Dimmeler S, Sauer S. Transcriptional heterogeneity of fibroblasts is a hallmark of the aging heart. *JCI Insight* 2019;**4**.
- Browaeys R, Saelens W, Saeys Y. NicheNet: modeling intercellular communication by linking ligands to target genes. *Nat Methods* 2020;**17**:159–162.
- Wang K, Li W, Yu Q, Guo B, Yang B, Zhang C, Li M, Li J, Hu S, Zheng Q, Song Z. High mobility group box 1 mediates interferon- $\gamma$ -induced phenotypic modulation of vascular smooth muscle cells. *J Cell Biochem* 2017;**118**:518–529.
- Michalek RD, Gerriets VA, Jacobs SR, Macintyre AN, MacIver NJ, Mason EF, Sullivan SA, Nichols AG, Rathmell JC. Cutting edge: distinct glycolytic and lipid oxidative metabolic programs are essential for effector and regulatory CD4<sup>+</sup> T cell subsets. *J Immunol* 2011;**186**:3299–3303.
- Bental M, Deutsch C. Metabolic changes in activated T cells: an NMR study of human peripheral blood lymphocytes. *Magn Reson Med* 1993;**29**:317–326.
- Pearce EL, Walsh MC, Cejas PJ, Harms GM, Shen H, Wang LS, Jones RG, Choi Y. Enhancing CD8 T cell memory by modulating fatty acid metabolism. *Nature* 2009;**460**:103–107.
- Dolejsi T, Delgado M, Schuetz T, Tortola L, Heinze KG, Hofmann U, Frantz S, Bauer A, Ruschitzka F, Penninger JM, Campos Ramos G, Haubner BJ. Adult T cells impair neonatal cardiac regeneration. *Eur Heart J* 2022;**43**:2698–2709.
- Finger S, Knorr M, Molitor M, Schüller R, Garlapati V, Waisman A, Brandt M, Münzel T, Bopp T, Kossmann S, Karbach S, Wenzel P. A sequential interferon gamma directed chemotactic cellular immune response determines survival and cardiac function post-myocardial infarction. *Cardiovasc Res* 2019;**115**:1907–1917.
- Nevers T, Salvador AM, Velazquez F, Ngwenyama N, Carrillo-Salinas FJ, Aronovitz M, Blanton RM, Alcaide P. Th1 effector T cells selectively orchestrate cardiac fibrosis in nonischemic heart failure. *J Exp Med* 2017;**214**:3311–3329.

35. Šestan M, Marinović S, Kavazović I, Cekinović Đ, Wuest S, Turk Wensveen T, Brzić I, Jonjić S, Konrad D, Wensveen FM, Polić B. Virus-Induced interferon- $\gamma$  causes insulin resistance in skeletal muscle and derails glycemic control in obesity. *Immunity* 2018;**49**:164–177.e6.
36. Lopaschuk GD, Karwi QG, Tian R, Wende AR, Abel ED. Cardiac energy metabolism in heart failure. *Circ Res* 2021;**128**:1487–1513.
37. Mogilenko DA, Shpynov O, Andhey PS, Arthur L, Swain A, Esaulova E, Brioschi S, Shchukina I, Kerndl M, Bambouskova M, Yao Z, Laha A, Zaitsev K, Burdett S, Gillilan S, Stewart SA, Colonna M, Artyomov MN. Comprehensive profiling of an aging immune system reveals clonal GZMK(+) CD8(+) T cells as conserved hallmark of inflammaging. *Immunity* 2021;**54**:99–115.e12.
38. Martini E, Cremonesi M, Panico C, Carullo P, Bonfiglio CA, Serio S, Jachetti E, Colombo MP, Condorelli G, Kalikourdis M. T cell costimulation blockade blunts age-related heart failure. *Circ Res* 2020;**127**:1115–1117.
39. Albig AR, Neil JR, Schiemann WP. Fibulins 3 and 5 antagonize tumor angiogenesis *in vivo*. *Cancer Res* 2006;**66**:2621–2629.
40. Hu B, Wu Z, Nakashima T, Phan SH. Mesenchymal-specific deletion of C/EBP $\beta$  suppresses pulmonary fibrosis. *Am J Pathol* 2012;**180**:2257–2267.
41. Gong GC, Song SR, Xu X, Luo Q, Han Q, He JX, Su J. Serpina3n is closely associated with fibrotic procession and knockdown ameliorates bleomycin-induced pulmonary fibrosis. *Biochem Biophys Res Commun* 2020;**532**:598–604.
42. Matthaei M, Meng H, Meeker AK, Eberhart CG, Jun AS. Endothelial *Cdkn1a* (p21) overexpression and accelerated senescence in a mouse model of Fuchs endothelial corneal dystrophy. *Invest Ophthalmol Vis Sci* 2012;**53**:6718–6727.
43. Hohberg M, Knöchel J, Hoffmann CJ, Chlench S, Wunderlich W, Alter A, Maroski J, Vorderwülbecke BJ, Da Silva-Azevedo L, Knudsen R, Lehmann R, Fiedorowicz K, Bongrazio M, Nitsche B, Hoepfner M, Styp-Rekowska B, Pries AR, Zakrzewicz A. Expression of ADAMTS1 in endothelial cells is induced by shear stress and suppressed in sprouting capillaries. *J Cell Physiol* 2011;**226**:350–361.
44. Helker CS, Eberlein J, Wilhelm K, Sugino T, Malchow J, Schuermann A, Baumeister S, Kwon HB, Maischein HM, Potente M, Herzog W, Stainier DY. Apelin signaling drives vascular endothelial cells toward a pro-angiogenic state. *Elife* 2020;**9**.
45. Filippov S, Koenig GC, Chun TH, Hotary KB, Ota I, Bugge TH, Roberts JD, Fay WP, Birkedal-Hansen H, Holmbeck K, Sabeh F, Allen ED, Weiss SJ. MT1-matrix Metalloproteinase directs arterial wall invasion and neointima formation by vascular smooth muscle cells. *J Exp Med* 2005;**202**:663–671.
46. Schiattarella GG, Rodolico D, Hill JA. Metabolic inflammation in heart failure with preserved ejection fraction. *Cardiovasc Res* 2021;**117**:423–434.
47. Ruiz-Meana M, Bou-Teen D, Ferdinandy P, Gyongyosi M, Pesce M, Perrino C, Schulz R, Sluijter JGP, Tocchetti CG, Thum T, Madonna R. Cardiomyocyte ageing and cardioprotection: consensus document from the ESC working groups cell biology of the heart and myocardial function. *Cardiovasc Res* 2020;**116**:1835–1849.
48. Reinhardt RL, Liang HE, Bao K, Price AE, Mohrs M, Kelly BL, Locksley RM. A novel model for IFN- $\gamma$ -mediated autoinflammatory syndromes. *J Immunol* 2015;**194**:2358–2368.
49. Reifenberg K, Lehr HA, Torzewski M, Steige G, Wiese E, Küpper I, Becker C, Ott S, Nüsser P, Yamamura K, Rechtsteiner G, Wargner T, Pautz A, Kleinert H, Schmidt A, Pieske B, Wenzel P, Münzel T, Löhler J. Interferon-gamma induces chronic active myocarditis and cardiomyopathy in transgenic mice. *Am J Pathol* 2007;**171**:463–472.
50. Wong N, Fam BC, Cempako GR, Steinberg GR, Walder K, Kay TW, Proietto J, Andrikopoulos S. Deficiency in interferon-gamma results in reduced body weight and better glucose tolerance in mice. *Endocrinology* 2011;**152**:3690–3699.
51. Deng Y, Xie M, Li Q, Xu X, Ou W, Zhang Y, Xiao H, Yu H, Zheng Y, Liang Y, Jiang C, Chen G, Du D, Zheng W, Wang S, Gong M, Chen Y, Tian R, Li T. Targeting mitochondria-inflammation circuit by  $\beta$ -hydroxybutyrate mitigates HFpEF. *Circ Res* 2021;**128**:232–245.
52. Nunes JPS, Andrieux P, Brochet P, Almeida RR, Kitano E, Honda AK, Iwai LK, Andrade-Silva D, Goudenège D, Alcântara Silva KD, Vieira RS, Levy D, Bydlowski SP, Gallardo F, Torres M, Bocchi EA, Mano M, Santos RHB, Bacal F, Pomerantzeff P, Laurindo FRM, Teixeira PC, Nakaya HI, Kalil J, Procaccio V, Chevillard C, Cunha-Neto E. Co-Exposure of cardiomyocytes to IFN- $\gamma$  and TNF- $\alpha$  induces mitochondrial dysfunction and nitro-oxidative stress: implications for the pathogenesis of chronic chagas disease cardiomyopathy. *Front Immunol* 2021;**12**:755862.
53. Ren Z, Yu P, Li D, Li Z, Liao Y, Wang Y, Zhou B, Wang L. Single-cell reconstruction of progression trajectory reveals intervention principles in pathological cardiac hypertrophy. *Circulation* 2020;**141**:1704–1719.
54. Franks A, Airolidi E, Slavov N. Post-transcriptional regulation across human tissues. *PLoS Comput Biol* 2017;**13**:e1005535.

## Translational perspective

Aging is a major risk factor for heart failure, but the mechanisms underlying this susceptibility remain unknown. In the present study, we provide novel evidence that, with aging, the T cell compartment undergoes clonal expansion with a pro-inflammatory bias, exposing the myocardium to chronic IFN- $\gamma$  signaling, which can recapitulate some inflammatory and metabolic shifts typically seen in failing hearts. Though physiological aging is not a disease entity, the age-related cardio-immune alterations described herein may help explain how advanced age poses an increased risk for the development of heart failure.